Journal of Organometallic Chemistry 695 (2010) 809–815

Contents lists available at ScienceDirect

Journal of Organometallic Chemistry

journal homepage: www.elsevier.com/locate/jorganchem

Synthesis and characterization of $(CH{=}CH)_n$-bridged (n = 1, 2, 3) heterobimetallic and trimetallic ferrocene–ruthenium complexes

Fang Liu, Xiang Hua Wu, Jian-Long Xia, Shan Jin, Guang-Ao Yu, Sheng Hua Liu *

Key Laboratory of Pesticide and Chemical Biology, Ministry of Education, College of Chemistry, Central China Normal University, Wuhan 430079, PR China

ARTICLE INFO

Article history:
Received 27 October 2009
Received in revised form 16 December 2009
Accepted 17 December 2009
Available online 28 December 2009

Keywords:
Synthesis
Heterobinuclear
Ferrocene
Ruthenium vinyl complexes
Electrochemistry

ABSTRACT

A series of heterobinuclear ferrocene–ruthenium complexes $Fc(CH{=}CH)_nRuCl(CO)(PMe_3)_3$ (n = 1, **3**; n = 2, **12**), $Fc(CH{=}CH)RuCl(CO)(Py)(PPh_3)_2$ (**4**), and trimetallic $Fc(CH{=}CH)RuCl(CO)(PPh_3)_2(Py{-}E{-}(CH{=}CH)Fc)$ (**6**) have been prepared. The length of the molecular rods is extended by successive insertion of CH=CH spacers in the bridging ligands or the ancillary ligands. The respective products have been fully characterized and the structures of **3** and **12** have been established by X-ray crystallography. Electrochemical studies have revealed that ethenyl heterobimetallic complexes display two successive one-electron processes, and that intermetallic electronic communication between the two endgroups is attenuated with the increase of the length of the conjugated bridge. The electrochemical behavior of the trimetallic complex reveals strong electronic communication between ruthenium and ferrocene transmitted through the ethenyl bridge, however, it also reveals a very weak interaction between ruthenium and ferrocene transmitted through the (E)–CH=CH–Py bridge.

1. Introduction

Considerable attention has been paid to studying homobimetallic complexes in which two equivalent metals are bonded through unsaturated bridges and most of the information on electronic communication comes from investigations on this class of compounds [1–19]. Heterometallic complexes, however, are asymmetric systems. This asymmetry means that the heterometallic complexes may have second-order NLO prosperities. Hetero-bimetallic complexes may have second-order NLO properties [20]. In fact, hetero-bimetallic complexes related to $(CH)_x$-bridged bimetallic complexes such as $[(CO)_3M{=}C(OCH_3){-}(CH{=}CH)_n{-}(C_5H_4)Fe(C_5H_5)$, M = W, Cr, n = 1–4] have been synthesized, and they have high β values [21].

Previously, we reported $(CH{=}CH)_3$-bridged heterobimetallic ferrocene–ruthenium complexes and found that the metals linked through the $(CH{=}CH)_3$ bridge interacted with each other [18]. In this paper, we focus further on the $(CH{=}CH)_n$-bridged (n = 1, 2, 3) ferrocene–ruthenium complexes and investigate how the length of the bridge, the nature of the ancillary ligands bound to the metal, and the coordination mode affect the intermetallic electronic communication in the complexes.

2. Results and discussion

2.1. Synthesis of FcCH=CHC≡CH (10)

The general synthetic route for the preparation of monometallic, heterobimetallic and trimetallic complexes is outlined in Scheme 1. The aldehyde FcCHO (**7**) underwent a Wittig reaction with the triphenylphosphonium bromide **8** to give the compound $FcCH{=}CHC{\equiv}CSiMe_3$ (**9**). The ferrocenyl-derived alkynyl compound **10** was obtained by reaction of **9** with Bu_4NF, which can be purified by chromatography on silica gel.

2.2. Synthesis and characterization of heterometallic complexes

The insertion products $FcCH{=}CHRu(CO)Cl(PPh_3)_2$ (**2**) and $FcCH{=}CHCH{=}CHRu(CO)Cl(PPh_3)_2$ (**11**) are obtained by reaction of $RuH(CO)Cl(PPh_3)_3$ with $FcC{\equiv}CH$ (**1**) [22], and $FcCH{=}CHC{\equiv}CH$ (**10**), respectively. The two compounds were characterized by NMR and elemental analysis. The ^{31}P NMR spectrum (in $CDCl_3$) of **2** displayed a signal at 31.68 ppm, as did compound **11** (32.18 ppm), which is similar to compound **14** [18] and typical for RuCl(E)–CH=CHR)(CO)$(PPh_3)_2$ [23].

Compounds **2** and **11** undergo a ligand-exchange reaction with PMe_3 to give the relevant six-coordinated complexes $FcCH{=}CHRu(CO)Cl(PMe_3)_3$ (**3**) and $FcCH{=}CHCH{=}CHRu(CO)Cl(PMe_3)_3$ (**12**), respectively. The PMe_3 ligands in **3** and **12** are meridionally coordinated to ruthenium, as indicated by an AM_2 pattern in the $^{31}P\{^1H\}$ NMR spectrum. The six-coordinated addition complex

* Corresponding author. Tel./fax: +86 27 67867725.
E-mail address: chshliu@mail.ccnu.edu.cn (S.H. Liu).

0022-328X/$ - see front matter © 2009 Elsevier B.V. All rights reserved.
doi:10.1016/j.jorganchem.2009.12.019

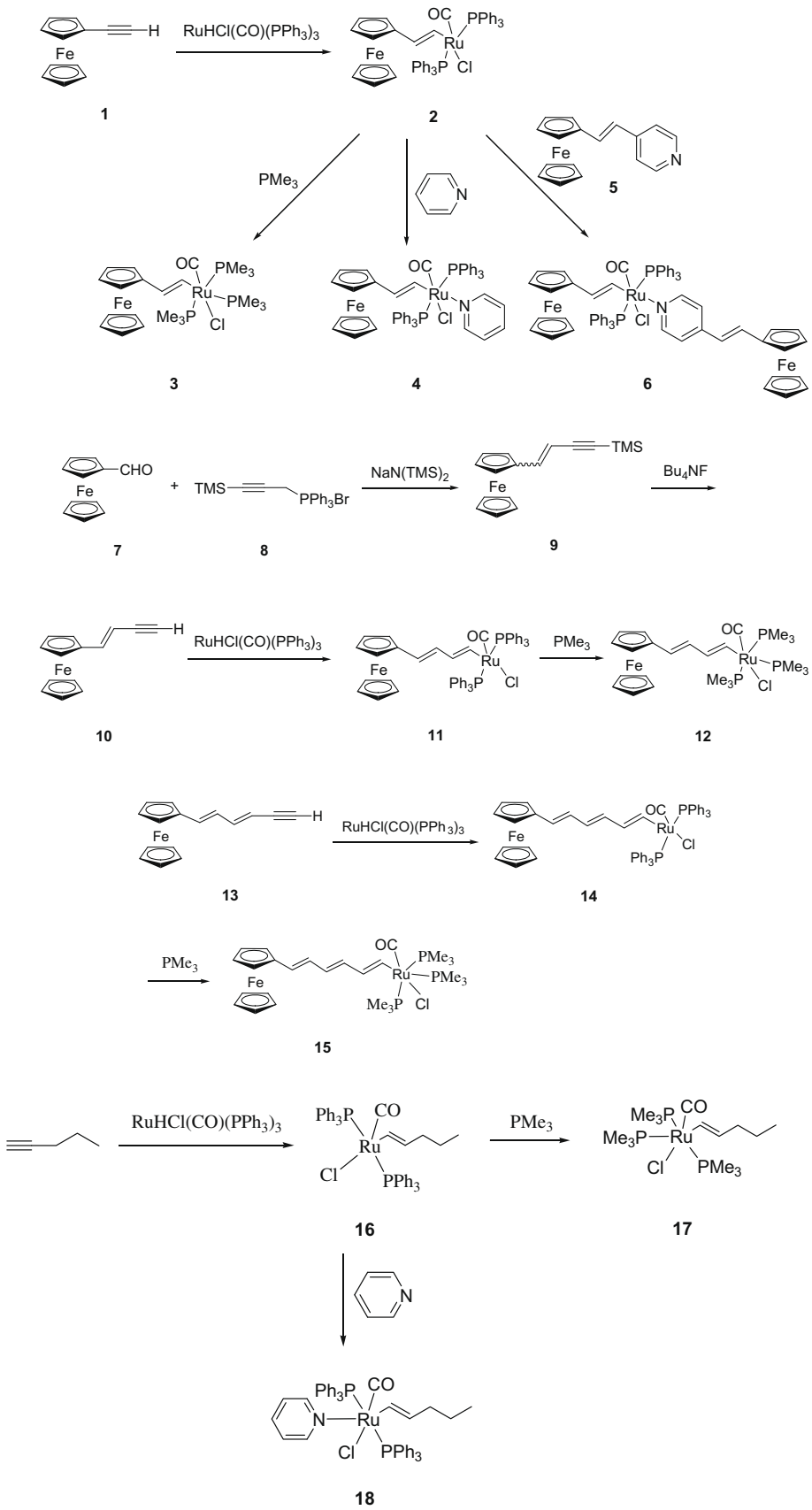
RuHCl(CO)(PPh3)3
PMe3
NaN(TMS)2
Bu4NF
1
2
3
4
5
6
7
8
9
10
11
12
13
14
15
16
17
18

Scheme 1.

FcCH=CHRu(CO)Cl(Py)$(PPh_3)_2$ (**4**) was obtained by reaction of compound **2** with pyridine (Py).

The compound Fc–(*E*)–CH=CH–Py (**5**) offers both a sp^2–π system and a nitrogen-like lone pair for bonding to metal centers and should be useful in the assembly of multi-metallic complexes. Reaction of Fc–(*E*)–CH=CH–Py (**5**) with compound **2** gives the corresponding six-coordinated three-center complex FcCH=CHRu(CO)Cl$(PPh_3)_2$(Py–CH=CH–(*E*)–Fc) (**6**).

The ^{1}H NMR spectra (in $CDCl_3$) of **3**, **4**, **10**, **11**, and **12** showed the Fc–CH proton signal with a big *J*(HH)coupling constant, which are 15.0 Hz (**3**), 15.6 Hz (**4**), 15.6 Hz (**10**), 15.6 Hz (**11**), and 15.0 Hz (**12**). The magnitude of the *J*(HH)coupling constant indicates that the two vinylic protons (Fc–CH=CH) are in a *trans* geometry. The ^{1}H NMR spectra (in $CDCl_3$) of **3** and **12** showed the Ru–CH proton signal with a big *J*(HH)coupling constant, which are 15.2 Hz (**3**) and 15.2 Hz (**12**). The magnitude of the *J*(HH)coupling constant indicates that the two vinylic protons (Ru–CH=CH) are in a *trans* geometry and that the acetylene is *cis*-inserted into the Ru–H bond.

2.3. X-ray structures of 3 and 12

The molecular structures of **3** and **12** were determined by X-ray crystallography. The crystallographic details are given in Table 1. Selected bond distances and angles for **3** and **12** are presented in Table 2. The molecular structures of **3** and **12** are depicted in Figs. 1 and 2, respectively. The complexes **3** and **12** contain a ferrocenyl moiety which has the cyclopentadienyl ring substituted with a CH=CH group or a CH=CHCH=CH group linked to a ruthenium center, respectively. In the ferrocene moiety, the dihedral angle of the substituted cyclopentadienyl ring and the unsubstituted one in complex **3** is 3.64°, which is bigger than that of 0.42° in complex **12**. All of the olefinic double bonds in **3** and **12** are in a *trans* geometry. The ruthenium center is a distorted octahedron with three meridionally bound PMe_3 ligands. The vinyl group is *trans* to a PMe_3 ligand and the CO group is *trans* to the chloride group. The overall geometry around the ruthenium center is closely related to the bimetallic ruthenium complex Fc(μ–CH=CHCH=CHCH=CH)RuCl(CO)$(PMe_3)_3$ [18].

Table 1
Crystal data, data collection, and refinement parameters for **3** and **12**.

	3	12
Formula	$C_{22}H_{38}ClFeOP_3Ru$	$C_{24}H_{40}ClFeOP_3Ru{\cdot}CH_2Cl_2$
Formula weight	603.80	714.77
T (K)	150(2)	298(2)
Crystal system	Monoclinic	Monoclinic
Space group	*P*2(1)/*c*	*P*2(1)/*n*
a (Å)	10.8484(12)	13.9345(3)
b (Å)	8.4672(9)	8.6398(2)
c (Å)	29.968(3)	27.1934(6)
α (°)	90	90
β (°)	94.394(2)	90.8120(10)
γ (°)	90	90
V (Å^{-3})	2744.7(5)	3273.52(13)
Z	4	4
D_{calcd} (g cm^{-3})	1.461	1.450
Crystal size (mm)	0.13 × 0.10 × 0.10	0.15 × 0.13 × 0.10
F(0 0 0)	1240	1464
Diffractometer	KappaCCD	KappaCCD
Radiation	MoK/*a*	MoK/*a*
Absorption coefficient (mm^{-1})	1.362	1.312
θ range (°)	1.36–27.00	1.63–26.00
hkl range	−13 to 12 −10 to 10 −38 to 38	−10 to 17 −10 to 10 −33 to 32
Total number of reflections	30054	18910
Number of unique reflections	5961	6411
Number of observed reflections [$I > 2\sigma(I)$]	5437	4294
Number of restraints/parameters	30/302	0/316
a, *b* for *W*[a]	0.0385, 1.6383	0.0467, 0.0000
Final *R*	0.0320	0.0595
R_w	0.0720	0.1104
R (all date)	0.0355	0.0979
R_w (all date)	0.0735	0.1216
Goodness-of-fit (GOF) on F^2	1.050	0.991
Largest difference in peak, hole (e Å^{-3})	1.008 and −0.745	0.722 and −0.382

[a] $W = 1/[\sigma^2(F_o)^2 + (aP)^2 + bP]$, where $P = (F_o^2 + F_c^2)/3$.

Table 2
Selected bond lengths (Å) and angles (°) for **3** and **12**.

	3	12
C(1)–C(11)	1.472(3)	1.464(7)
C(11)–C(12)	1.337(3)	1.330(7)
C(12)–C(13)		1.438(7)
C(13)–C(14)		1.326(6)
C(12)–Ru(1)	2.097(2)	
C(14)–Ru(1)		2.094(5)
C(1)–C(11)–C(12)	125.1(2)	126.8(5)
C(11)–C(12)–C(13)		126.4(5)
C(12)–C(13)–C(14)		125.2(5)
C(11)–C(12)–Ru(1)	131.6(2)	
C(13)–C(14)–Ru(1)		131.6(4)

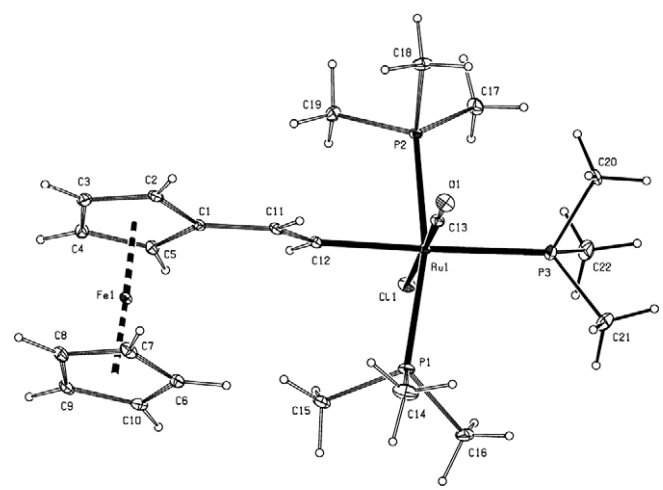

Fig. 1. Molecular structure of **3**. For the disordered P(3)Me_3, only one set of the disordered atoms [C(20), C(21), and C(22)] are shown.

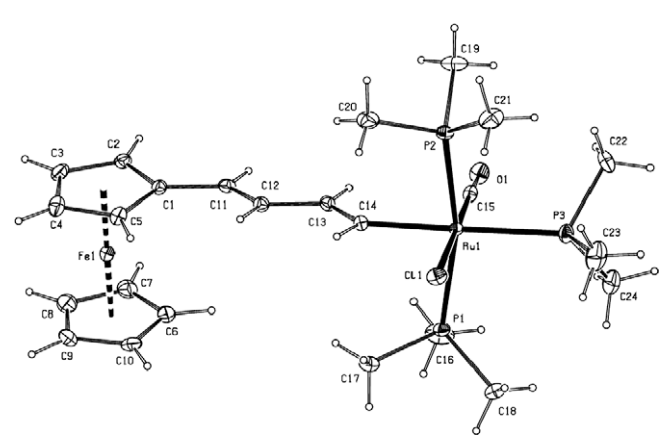

Fig. 2. Molecular structure of **12**, solvent is omitted for clarity.

2.4. Electrochemistry

The redox behavior of the mononuclear complexes (**1**, **10**, **17**, and **18**), binuclear complexes (**3**, **4**, **12**, and **15**), and the trinuclear complex (**6**) (1 mM in CH_2Cl_2) has been investigated by cyclic voltammetric and square-wave voltammetric techniques with 0.1 M n-Bu_4NPF_6 as the supporting electrolyte; pertinent data are compiled in Tables 3 and 4. Cyclic voltammograms of the related monometallic iron (**1**) and ruthenium (**17**) complexes gave only one oxidation. Heterobimetallic complex **3** undergoes two consecutive one-electron oxidation processes separated by 0.86 V (Fig. 3, Table 3). The first oxidation wave at 0.00 V in the cyclic voltammogram of complex **3** is tentatively ascribed to the ferrocene–ferrocenium couple. Substitution of the end hydrogen in the iron complex **1** by the ruthenium end group renders oxidation 0.44 V more favorable. The second oxidation, which should have more ruthenium character, is about 0.26 V less unfavorable than that of the monometallic ruthenium complex **17**. This can be attributed to the strong electronic communications between the iron end group and the ruthenium end group [1c].

Heterobimetallic complexes **3**, **12**, and **15**, in which PMe_3 are ancillary ligands bound to the metal, undergo two consecutive one-electron oxidation processes, giving rise to redox waves A and B (Fig. 4, Table 3). The first oxidation occurs at the iron center, the second occurring at ruthenium, corresponding to oxidation of $Fe^{II}Ru^{II}$ to $Fe^{III}Ru^{II}$ and then of $Fe^{III}Ru^{II}$ to $Fe^{III}Ru^{III}$. The first oxidation waves at 0.00, 0.04, and 0.09 V in the cyclic voltammogram of complexes **3**, **12**, and **15** respectively, are ascribed to the ferrocene–ferrocenium couples. The second oxidation waves, which are ascribed to the Ru^{II}–Ru^{III} couples, are at 0.86 V for **3**, 0.46 V for **12**, and 0.27 V for **15** (the ferrocene/ferrocenium redox couple was located at 0.27 V under the experimental condition of Ref. [19]). Comparing with complexes **12** and **15**, complex **3** has the highest second oxidation potential, which is attributed to the shortest distance between ferrocene and the ruthenium atom. The higher charge of ferrocenium transfers easily to the ruthenium atom after the ferrocene in complex **3** is oxidized; therefore the ruthenium atom is oxidized at a higher oxidation potential than the ruthenium atoms in complexes **12** and **15**. It is found that the oxidation of the ruthenium atoms in the complexes occurs more easily with the increased length of the bridge ligands. This indicates that the interaction between ferrocene and the ruthenium atom is reduced with the increasing length of the conjugated bridge.

Comparing the $\Delta E_{1/2}$ values of complexes **3**, **12**, and **15** could further support the above conclusion. In complexes **3**, **12**, and **15** with ethenyl (CH=CH)n (n = 1, 2, 3) as a spacer, the $\Delta E_{1/2}$ values are 0.86, 0.42 and 0.18 V, respectively (Table 4). The large potential separation ($\Delta E_{1/2}$ = 0.86 V) in complex **3** between the two one-

Table 3
Electrochemical data for PMe_3-containing complexes.[a]

Compound	$E^A_{1/2}$ (V)	$E^B_{1/2}$ (V)	$\Delta E_{1/2}$ (V)
1	0.44	–	–
3	0.00	0.86	0.86
10	0.31	–	–
12	0.04	0.46	0.42
15	0.09	0.27	0.18
17	–	0.58	–

[a] Cyclic voltammograms recorded in 0.1 M Bu_4NPF_6 in CH_2Cl_2, 0.1 V s^{-1}, Pt electrode, V vs. SCE (cf. Fc/Fc^+ 0.270 V vs. SCE).

Table 4
Electrochemical data for Py-containing complexes.[a]

Compound	$E_{1/2}$(A) (V)	$E_{1/2}$(B) (V)	$E_{1/2}$(C) (V)	E(C) − E(A)
4	−0.08	–	0.76	0.84
5	–	0.26	–	–
6	−0.09	0.27	0.78	0.87
18			0.51	

[a] Cyclic voltammograms recorded in 0.1 M Bu_4NPF_6 in CH_2Cl_2, 0.1 V s^{-1}, Pt electrode, V vs. SCE (cf. Fc/Fc^+ 0.270 V vs. SCE).

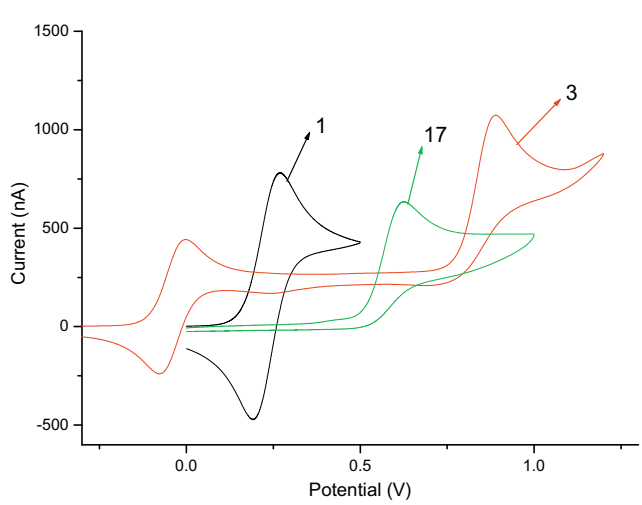

Fig. 3. Cyclic voltammograms (CVs) of complexes **1**, **3**, and **17** in CH_2Cl_2/Bu_4NPF_6 at υ = 0.1 V s^{-1}. Potentials are given relative to the $Ag|Ag^+$ standard.

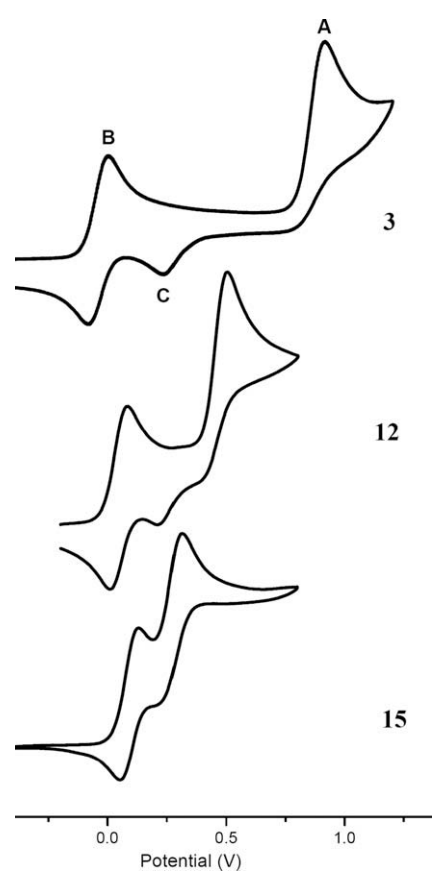

Fig. 4. Cyclic voltammograms (CVs) of complexes **3**, **12**, and **15** in CH_2Cl_2/Bu_4NPF_6 at υ = 0.1 V s^{-1}. Potentials are given relative to the $Ag|Ag^+$ standard.

electron processes reflects a remarkable electronic delocalization along the ethenyl bridge. By comparison of the above $\Delta E_{1/2}$ values, it can be seen that electronic communication is rapidly attenuated with a successive insertion of two and three ethenyl units into the bridge.

Complexes **3** and **12** exhibit an irreversible wave at 0.21 and 0.24 V (C), respectively, which is dependent on the potential window: C disappeared when the potential sweep was limited to 0.4 V (Fig. 4). Similar phenomenon has been recently reported by Ren and co-workers [24].

The redox behavior of complex **4**, in which PPh_3 and Py are attached to the metal center, is similar to complex **3** (Fig. 5, Table 4). The $\Delta E_{1/2}$ value in complex **4** is 0.84 V (Table 4). This rather large $\Delta E_{1/2}$ for **4** is indicative of strong electronic communication transmitted through the ethenyl bridge. In order to gain an understanding of the charge-transfer processes of the ferrocene–ruthenium through different bonding modes, the redox behavior of the three-center complex **6** has been investigated by cyclic voltammetry and square-wave voltammetry (Table 4). Complex Fc–(*E*)–CH=CH–Py undergoes a reversible one-electron oxidation process at 0.26 V, while complex **18** presents a irreversible one-electron redox wave at 0.51 V. Complex **6** undergoes three consecutive one-electron oxidation processes, giving rise to redox waves A′, B′, and C′ (Table 4). In complex **6**, the first oxidation wave lies at −0.09 V, the second oxidation wave at 0.27 V, and the third oxidation wave at 0.78 V (Fig. 4). Comparing the CV data (Table 4) with those of the related species, the first oxidation occurs at the iron center (A′), the second oxidation occurs at the iron center (B′) the third oxidation occurs at the ruthenium (C′). It is found that the second oxidation value is nearly equivalent with the value of complex Fc–(*E*)–CH=CH–Py. The values of the first and the third oxidation are nearly equivalent to the values of complex **4**. This reveals strong electronic communication between ruthenium and ferrocene transmitted through the ethenyl bridge, however, a very weak interaction between ruthenium and ferrocene is transmitted through the (*E*)–CH=CH–Py bridge. The results indicate that the complexes, which contain a conjugated bridge linking metal atoms by σ metal–carbon bonds show much stronger electronic communication between metal atoms than the complexes in which a bridge links the metal atoms by a dative bond. This is in good agreement with the conclusion reported by Paul and Lapinte [25] and Fillaut et al. [26].

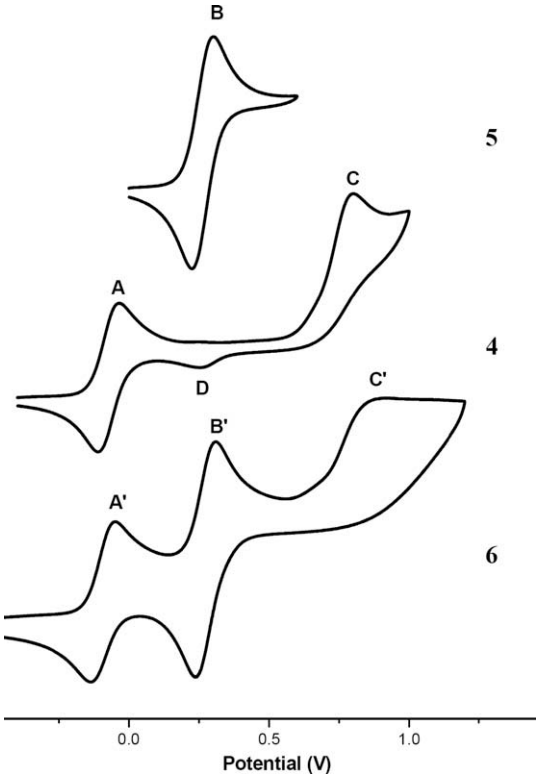

Fig. 5. Cyclic voltammograms (CVs) of complexes **4**, **5**, and **6** in CH_2Cl_2/Bu_4NPF_6 at $\upsilon = 0.1$ V s^{-1}. Potentials are given relative to the Ag|Ag^+ standard.

3. Conclusions

We have reported here the synthesis, characterization, and electrochemical properties of a series of ferrocene–ruthenium complexes. Electrochemical studies have revealed that ethenyl heterobimetallic complexes display two successive one-electron processes and that intermetallic electronic communication between the two end-groups is attenuated with the increase of the length of the conjugated bridge. The electrochemical behavior of the trimetallic complex reveals strong electronic communication between ruthenium and ferrocene transmitted through the ethenyl bridge and a very weak interaction between ruthenium and ferrocene transmitted through the (*E*)–CH=CH–Py bridge.

4. Experimental section

4.1. General materials

All manipulations were carried out at room temperature under a nitrogen atmosphere using standard Schlenk techniques, unless otherwise stated. Solvents were pre-dried, distilled and degassed prior to use, except those for spectroscopic measurements, which were of spectroscopic grade. The starting materials $RuHCl(CO)(PPh_3)_3$ [27], TMS–C≡CCH_2PPh_3Br [28], ethynylferrocene [22], formylferrocene [29], and Fc–(*E*)–CH=CH–Py [30] were prepared according to literature methods, and complex **15** [18] was also prepared according to literature method.

4.2. Synthesis of FcCH=CHRuCl(CO)(PPh$_3$)$_2$ (**2**)

To suspension of $RuHCl(CO)(PPh_3)_3$ (0.44 g, 0.46 mmol) in CH_2Cl_2 (30 mL) was slowly added a solution of **1** (0.11 g, 0.52 mmol) in CH_2Cl_2 (10 mL). The reaction mixture was stirred for 30 min to give a red solution. The reaction mixture was filtered through a column of Celite. The volume of the filtrate was reduced to ca. 5 mL under vacuum. Addition of hexane (50 mL) to the residue produced a red solid, which was collected by filtration, washed with hexane, and dried under vacuum. Yield: 0.36 g, 86%. *Anal.* Calc. for $C_{49}H_{41}ClFeOP_2Ru$: C, 65.38; H, 4.59. Found: C, 65.53; H, 4.42%. ^{31}P NMR (240 MHz, $CDCl_3$): δ 31.68 (s). ^1H NMR (600 MHz, $CDCl_3$): δ 3.79 (s, 5H, C_5H_5), 3.87 (s, 2H, $C_5H_2H_2C$=), 3.96 (s, 2H, $C_5H_2H_2C$=), 5.41 (d, J = 13.2 Hz, 1H, FcC*H*=), 7.35–7.57 (m, 30H, *Ph*), 7.72 (d, J = 13.2 Hz, 1H, Ru–C*H*).

4.3. Synthesis of FcCH=CHRuCl(CO)(PMe$_3$)$_3$ (**3**)

To a solution of complex **2** (0.18 g, 0.20 mmol) in CH_2Cl_2 (30 mL) was added a 1.0 M THF solution of PMe_3 (2.0 mL, 2.0 mmol). The reaction mixture was stirred for 15 h. The solvent of the reaction mixture was removed under vacuum. The residue was purified by column chromatography (silica gel, eluted with 20/80 acetone/petroleum ether) to give a yellow solid. Yield: 0.08 g, 70%. *Anal.* Calc. for $C_{22}H_{38}ClFeOP_3Ru$: C, 43.76; H, 6.34. Found: C, 43.38; H, 6.01%. ^{31}P NMR (240 MHz, $CDCl_3$): δ −18.46 (t, J = 21.4 Hz, *P*Me$_3$), −7.08 (d, J = 21.4 Hz, *P*Me$_3$). ^1H NMR (600 MHz, $CDCl_3$): δ 1.43 (t, J = 3.0 Hz, 18H, P*Me*$_3$), 1.47 (d, J = 7.2 Hz,

9H, P*Me*$_3$), 4.06 (s, 5H, C_5H_5), 4.09 (s, 2H, $C_5H_2H_2C$=), 4.27 (s, 2H, $C_5H_2H_2C$=), 6.17 (d, *J* = 15.0 Hz, 1H, FcC*H*=), 7.35 (ddt, J_{HH} = 15.2 Hz, J_{PH} = 7.0 Hz, J_{PH} = 3.5 Hz, 1H, Ru–*H*). ^{13}C NMR (150 MHz, $CDCl_3$): δ 16.45 (t, *J* = 14.8 Hz, P*Me*$_3$), 22.12 (d, *J* = 20.2 Hz, P*Me*$_3$), 64.30, 66.66, 68.04, 91.64 (s, C_5H_5, C_5H_4), 129.84 (s, FcCH=), 159.79 (s, Ru–CH), 202.42 (br, *C*O).

4.4. Synthesis of FcCH=CHRu(CO)Cl(PPh$_3$)$_2$(Py) (**4**)

A mixture of complex **2** (0.18 g, 0.20 mmol) and pyridine (0.2 mL, 2.5 mmol) in CH_2Cl_2 (20 mL) was stirred for 30 min. The solution was filtered through a column of Celite. The volume of the filtrate was reduced to ca. 2 mL under vacuum. Addition of hexane (15 mL) to the residue produced a yellow solid, which was collected by filtration, washed with hexane, and dried under vacuum. Yield: 0.17 g, 87%. *Anal.* Calc. for $C_{54}H_{46}ClFeNOP_2Ru$: C, 66.23; H, 4.73. Found: C, 66.16; H, 4.77%. ^{31}P NMR (240 MHz, $CDCl_3$): δ 25.73 (s). ^{1}H NMR (600 MHz, $CDCl_3$): δ 3.76 (s, 5H, C_5H_5), 3.80 (s, 2H, $C_5H_2H_2C$=), 3.96 (s, 2H, $C_5H_2H_2C$=), 5.56 (d, *J* = 15.6 Hz, 1H, FcC*H*=), 6.59 (br, 2H, *Py*), 7.12–7.30 (m, 19H, 18H *Ph* and 1H *Py*), 7.62 (m, 13H, 12H *Ph* and Ru–*H*), 8.47 (br, 2H, *Py*).

4.5. Synthesis of FcCH=CHRu(CO)Cl(PPh$_3$)$_2$(Fc–(E)–CH=CH–Py) (**5**)

A mixture of complex **2** (0.18 g, 0.20 mmol) and Fc–(*E*)–CH=CH–Py (0.06 g, 0.21 mmol) in CH_2Cl_2 (20 mL) was stirred for 15 h. The solution was filtered through a column of Celite. The volume of the filtrate was reduced to ca. 5 mL under vacuum. Addition of hexane (50 mL) to the residue produced a red solid, which was collected by filtration, washed with hexane, and dried under vacuum. Yield: 0.21 g, 90%. *Anal.* Calc. for $C_{66}H_{56}ClFe_2NOP_2Ru$: C, 66.65; H, 4.75. Found: C, 66.73; H, 4.99%. ^{31}P NMR (240 MHz, $CDCl_3$): δ 25.47 (s). ^{1}H NMR (600 MHz, $CDCl_3$): δ 3.75 (s, 5H, C_5H_5), 3.94 (s, 4H, C_5H_4), 4.16 (s, 5H, C_5H_5), 4.39 (s, 2H, $C_5H_2H_2$), 4.50 (s, 2H, $C_5H_2H_2$), 5.59 (d, *J* = 15.2 Hz, 1H, FcC*H*=), 6.36 (d, *J* = 15.6 Hz, 1H, PyC*H*=CH), 6.52 (br, 2H, *Py*), 6.93 (d, *J* = 15.6 Hz, 1H, PyCH=C*H*), 7.18–7.55 (m, 31H, 30H *Ph* and Ru–*H*), 8.29 (br, 2H, *Py*). ^{13}C NMR (150 MHz, $CDCl_3$): δ 63.80, 66.36, 67.49, 69.39, 70.12, 80.96 (s, C_5H_5, C_5H_4), 121.80, 127.34, 128.99, 132.55, 132.75, 132.95, 133.12, 133.60, 134.30, 144.18 (s, *Ph, Py,* CH=CH), 153.50 (s, Ru–CH), 203.75 (br, *C*O).

4.6. Synthesis of FcCH=CHC≡CH (**10**)

To a slurry of TMS–C≡CCH$_2$PPh$_3$Br (0.5 g, 1.1 mmol) in THF (20 mL) was added a 2.0 M THF solution of NaN(SiMe$_3$)$_2$ (0.7 mL, 1.4 mmol). The mixture was stirred for 30 min, and then a solution of the formylferrocene (0.2 g, 0.9 mmol) in THF (10 mL) was added slowly. The resulting solution was stirred for another 2 h, and then water (50 mL) was added. The layers were separated, and the aqueous layer was extracted with diethyl ether (3 × 30 mL). The combined organic layers were washed with a saturated aqueous solution of sodium chloride (2 × 10 mL), dried over Na_2SO_4, filtered, and then concentrated under rotary evaporation. The crude product was purified by column chromatography (silica gel, eluted with petroleum ether) to give compound **9**. Yield: 0.22 g, 81%. ^{1}H NMR (600 MHz, $CDCl_3$): δ 0.21 (s, 9H, SiMe$_3$), 4.14 (s, 5H, C_5H_5), 4.26 (s, 2H, $C_5H_2H_2C$=), 4.34 (s, 2H, $C_5H_2H_2C$=), 5.74 (d, *J* = 15.4 Hz, 1H, FcCH=C*H*), 6.82 (d, *J* = 15.3 Hz, 1H, FcC*H*=CH).

To a solution of compound **9** (0.17 g, 0.55 mmol) in THF (10 mL) was slowly added a 1.0 M THF solution of *n*-Bu$_4$NF (0.6 mL, 0.6 mmol) with stirring. After 2 h, the solvent was removed and the crude product was purified by column chromatography to give complex **10**. Yield: 0.11 g, 42%. *Anal.* Calc. for $C_{14}H_{12}Fe$: C, 71.22; H, 5.12. Found: C, 71.50; H, 5.01%. ^{1}H NMR (600 MHz, $CDCl_3$): δ 2.99 (s, 1H, ≡C*H*), 4.15 (s, 5H, C_5H_5), 4.29 (s, 2H, $C_5H_2H_2C$=), 4.37 (s, 2H, $C_5H_2H_2C$=), 5.71 (d, *J* = 15.6 Hz, 1H, FcCH=C*H*), 6.84 (d, *J* = 15.6 Hz, 1H, FcC*H*=CH). ^{13}C NMR (150 MHz, $CDCl_3$): δ 66.96, 69.35, 69.65, 81.06 (s, C_5H_5, C_5H_4), 77.36, 83.61 (s, C≡C), 103.47, 142.50 (s, CH=CH).

4.7. Synthesis of FcCH=CHCH=CHRuCl(CO)(PPh$_3$)$_2$ (**11**)

The synthesis is similar to **2**, with FcC≡CH being replaced by FcCH=CHC≡CH (**9**). Yellow solid, yield: 0.34 g, 79%. *Anal.* Calc. for $C_{51}H_{43}ClFeOP_2Ru$: C, 66.14; H, 4.68. Found: C, 66.45; H, 4.91%. ^{31}P NMR (240 MHz, $CDCl_3$): δ 32.18 (s). ^{1}H NMR (600 MHz, $CDCl_3$): δ 4.02 (s, 5H, C_5H_5), 4.12 (s, 2H, $C_5H_2H_2C$=), 4.20 (s, 2H, $C_5H_2H_2C$=), 5.25 (d, *J* = 15.6 Hz, 1H, FcC*H*=), 5.43 (m, 1H, FcCH=CHC*H*=), 6.08 (m, 1H, FcCH= C*H*CH=), 7.34–7.67 (m, 31H, 30H *Ph* and Ru–C*H*).

4.8. Synthesis of FcCH=CHCH=CHRuCl(CO)(PMe$_3$)$_3$ (**12**)

The synthesis is similar to **3**. Red solid, yield: 0.096 g, 76%. *Anal.* Calc. for $C_{24}H_{40}ClFeOP_3Ru$: C, 45.76; H, 6.40. Found: C, 45.90; H, 6.74%. ^{31}P NMR (240 MHz, $CDCl_3$): δ −19.08 (t, *J* = 21.4 Hz, *P*Me$_3$), −7.54 (d, *J* = 21.4 Hz, *P*Me$_3$). ^{1}H NMR (600 MHz, $CDCl_3$): δ 1.40 (t, *J* = 3.4 Hz, 18H, P*Me*$_3$), 1.49 (d, *J* = 7.8 Hz, 9H, P*Me*$_3$), 4.06 (s, 5H, C_5H_5), 4.14 (s, 2H, $C_5H_2H_2C$=), 4.30 (s, 2H, $C_5H_2H_2C$=), 5.81 (d, *J* = 15.0 Hz, 1H, FcC*H*=), 6.34 (m, 1H, FcCH=CHC*H*=), 6.43 (m, 1H, FcCH= C*H*CH=), 7.48 (ddt, J_{HH} = 15.2 Hz, J_{PH} = 7.2 Hz, J_{PH} = 3.6 Hz, 1H, Ru–C*H*). ^{13}C NMR (150 MHz, $CDCl_3$): δ 16.71 (t, *J* = 15.1 Hz, P*Me*$_3$), 20.07 (d, *J* = 20.1 Hz, P*Me*$_3$), 65.92, 67.91, 69.13, 85.89 (s, C_5H_5, C_5H_4), 128.47, 133.61, 137.71 (s, CH=CH), 170.37 (s, Ru–CH), 202.29 (br, *C*O).

4.9. Synthesis of C$_3$H$_7$CH=CHRuCl(CO)(PMe$_3$)$_3$ (**17**)

The synthesis is similar to **3**. Yellow solid, yield: 0.11 g, 73%. *Anal.* Calc. for $C_{15}H_{36}ClOP_3Ru$: C, 39.01; H, 7.86. Found: C, 39.13; H, 7.99%. ^{31}P NMR (240 MHz, $CDCl_3$): δ −18.94 (t, *J* = 21.4 Hz, *P*Me$_3$), −7.27 (d, *J* = 20.0 Hz, *P*Me$_3$). ^{1}H NMR (600 MHz, $CDCl_3$): δ 0.90 (t, *J* = 7.2 Hz, 3H, C*H*$_3$), 1.39 (m, 20H, P*Me*$_3$, CH$_3$C*H*$_2$CH$_2$), 1.43 (d, *J* = 6.6 Hz, 9H, P*Me*$_3$), 2.08 (m, 2H, CH$_3$CH$_2$C*H*$_2$), 5.41 (m, 1H, CH$_2$C*H*=), 6.65 (ddt, J_{HH} = 15.8 Hz, J_{PH} = 7.2 Hz, J_{PH} = 3.6 Hz, Ru–*H*). ^{13}C NMR (150 MHz, $CDCl_3$): δ 13.96 (s, CH$_3$), 16.15 (t, *J* = 15.1 Hz, P*Me*$_3$), 19.98 (d, *J* = 20.2 Hz, P*Me*$_3$), 22.99, 41.17 (s, CH$_3$CH$_2$CH$_2$, CH$_3$CH$_2$CH$_2$), 134.92 (s, CH$_2$CH=), 155.31 (s, Ru–CH), 202.33 (s, *C*O).

4.10. Synthesis of C$_3$H$_7$CH=CHRuCl(CO)(PPh$_3$)$_2$(Py) (**18**)

The synthesis is similar to **4**. Yellow solid, yield: 0.12 g, 68%. *Anal.* Calc. for $C_{47}H_{44}ClNOP_2Ru$: C, 67.42; H, 5.30. Found: C, 67.56; H, 5.73%. ^{31}P NMR (240 MHz, $CDCl_3$): δ 26.69 (s). ^{1}H NMR (600 MHz, $CDCl_3$): δ 0.66 (t, *J* = 7.2 Hz, 3H, C*H*$_3$), 1.05 (m, 2H, CH$_3$C*H*$_2$CH$_2$), 1.84 (m, 2H, CH$_3$CH$_2$C*H*$_2$), 4.78 (m, 1H, CH$_2$C*H*=), 6.58 (br, 2H, *Py*), 7.15–7.29 (m, 19H, 18H *Ph* and 1H *Py*), 7.59 (m, 13H, 12H *Ph* and Ru–*H*), 8.49 (br, 2H, *Py*).

4.11. Crystallographic details

Crystals suitable for X-ray diffraction were grown from a dichloromethane of solution **3** and **12** layered with hexane. A crystal with approximate dimensions of 0.13 × 0.10 × 0.10 mm^3 for **3** and 0.15 × 0.13 × 0.10 mm^3 for **12** was mounted on a glass fiber for diffraction experiment. Intensity data were collected on a Nonius Kappa CCD diffractometer with Mo Kα radiation (0.71073 Å) at room temperature. The structures were solved by a combination of direct methods (SHELXS-97 [31]) and Fourier difference techniques and refined by full-matrix least squares (SHELXL-97 [32]). All non-H atoms were refined anisotropically. The hydrogen atoms

were placed in the ideal positions and refined as riding atoms. Further crystal data and details of the data collection are summarized in Table 1. Selected bond distances and angles are given in Tables 2.

4.12. Physical Measurements

Elemental analyses (C, H, N) were performed by Vario ELIII CHNSO. ^{1}H, $^{13}C\{^{1}H\}$, and $^{31}P\{^{1}H\}$ NMR spectra were collected on a Varian MERCURY Plus 600 spectrometer (600 MHz). ^{1}H, ^{13}C NMR chemical shifts are relative to TMS, and ^{31}P NMR chemical shifts are relative to 85% H_3PO_4. UV–vis spectra were recorded on a PDA spectrophotometer by quartz cells with path length of 1.0 cm. The electrochemical measurements were performed on a CHI 660C potentiostat (CHI USA). A three-electrode one-compartment cell was used to containing the solution of the compound and supporting electrolyte in dry CH_2Cl_2. Deaeration of the solution was achieved by argon bubbling through the solution for about 10 min. before measurement. The ligand and electrolyte (Bu_4NPF_6) concentrations were typically 0.001 and 0.1 mol dm^{-3}, respectively. A 500 μm diameter platinum disc working electrode, a platinum wire counter electrode, and an Ag|Ag^{+} reference electrode were used. The Ag|Ag^{+} reference electrode contained an internal solution of 0.01 mol dm^{-3} $AgNO_3$ in acetonitrile and was incorporated to the cell with a salt bridge containing 0.1 mol dm^{-3} Bu_4NPF_6 in CH_2Cl_2. All electrochemical experiments were carried out under ambient conditions.

Acknowledgements

The authors acknowledge financial support from National Natural Science Foundation of China (Nos. 20572029, 2072039, and 20931006) and the Natural Science Foundation of Hubei Province (No. 2008CDB023).

Appendix A. Supplementary material

CCDC 751624 for complex **3** and CCDC 751625 for complex **12** contain the supplementary crystallographic data for this paper. These data can be obtained free of charge from The Cambridge Crystallographic Data Centre via www.ccdc.cam.ac.uk/data_request/cif. Supplementary data associated with this article can be found, in the online version. Supplementary data associated with this article can be found, in the online version, at doi:10.1016/j.jorganchem.2009.12.019.

References

[1] (a) R. Dembinski, T. Bartik, J.A. Gladysz, J. Am. Chem. Soc. 122 (2000) 810;
(b) S. Barlow, D. O'Hare, Chem. Rev. 97 (1997) 637;
(c) F. Paul, W.E. Meyer, L. Toupet, H. Jiao, J.A. Gladysz, C. Lapinte, J. Am. Chem. Soc. 122 (2000) 9405.
[2] J. Stahl, W. Mohr, L. de Quadras, T.B. Peters, J.C. Bohling, J.M. Martín-Alvarez, G.R. Owen, F. Hampel, J.A. Gladysz, J. Am. Chem. Soc. 129 (2007) 8282.
[3] T. Ren, G.-L. Xu, Comment. Inorg. Chem. 23 (2002) 355.
[4] G.-L. Xu, G. Zou, Y.-H. Ni, M.C. DeRosa, R.J. Crutchley, T. Ren, J. Am. Chem. Soc. 125 (2003) 10057.
[5] Y.H. Shi, G.T. Yee, G.B. Wang, T. Ren, J. Am. Chem. Soc. 126 (2004) 10552.
[6] A.S. Blum, T. Ren, D.A. Parish, S.A. Trammell, M.H. Moore, J.G. Kushmerick, G.-L. Xu, J.R. Deschamps, S.K. Pollack, R. Shashidhar, J. Am. Chem. Soc. 127 (2005) 10010.
[7] S. Rigaut, K. Costuas, D. Touchard, J.-Y. Saillard, S. Golhen, P.H. Dixneuf, J. Am. Chem. Soc. 126 (2004) 4072.
[8] S. Rigaut, C. Olivier, K. Costuas, S. Choua, O. Fadhel, J. Massue, P. Turek, J.-Y. Saillard, P.H. Dixneuf, D. Touchard, J. Am. Chem. Soc. 128 (2006) 5859.
[9] S. Ibn Ghazala, F. Paul, L. Toupet, T. Roisnel, P. Hapiot, C. Lapinte, J. Am. Chem. Soc. 128 (2006) 2463.
[10] S. Le Stang, F. Paul, C. Lapinte, Organometallics 19 (2000) 1035.
[11] Y. Tanaka, J.A. Shaw-Taberlet, F. Justaud, O. Cador, T. Roisnel, M. Akita, J.-R. Hamon, C. Lapinte, Organometallics 28 (2009) 4656.
[12] F. de Montigny, G. Argouarch, K. Costuas, J.-F. Halet, T. Roisnel, L. Toupet, C. Lapinte, Organometallics 24 (2005) 4558.
[13] L.-B. Gao, L.-Y. Zhang, L.-X. Shi, Z.-N. Chen, Organometallics 24 (2005) 1678.
[14] L.-B. Gao, S.H. Liu, L.-Y. Zhang, L.-X. Shi, Z.-N. Chen, Organometallics 25 (2006) 506.
[15] L.-B. Gao, J. Kan, Y. Fan, L.-Y. Zhang, S.H. Liu, Z.-N. Chen, Inorg. Chem. 46 (2007) 5651.
[16] J.-L. Xia, X.H. Wu, Y. Lu, G. Chen, S. Jin, G.-A. Yu, S.H. Liu, Organometallics 28 (2009) 2701.
[17] X.H. Wu, S. Jin, J.H. Liang, Z.Y. Li, G.-A. Yu, S.H. Liu, Organometallics 28 (2009) 2450.
[18] P. Yuan, S.H. Liu, W. Xiong, J. Yin, G. Yu, H.Y. Sung, I.D. Williams, G. Jia, Organometallics 24 (2005) 1452.
[19] S.H. Liu, Q.Y. Hu, P. Xue, T.B. Wen, I.D. Williams, G. Jia, Organometallics 24 (2005) 769.
[20] (a) S.D. Bella, Chem. Soc. Rev. 30 (2001) 355;
(b) M.J. Macgregor, G. Hogarth, A.L. Thompson, J.D.E.T. Wilton-Ely, Organometallics 28 (2009) 197;
(c) K. Kowalski, M. Linseis, R.F. Winter, M. Zabel, S. Záli, H. Kelm, H.-J. Krüger, B. Sarkar, W. Kaim, Organometallics 28 (2009) 4196.
[21] K.N. Jayaprakash, P.C. Ray, I. Matsuoka, M.M. Bhadbhade, V.G. Puranik, P.K. Das, H. Nirshihara, A. Sarkar, Organometallics 18 (1999) 3851.
[22] J. Polin, H. Schottenberger, Org. Synth. 73 (1996) 262.
[23] M.R. Torres, A. Vegas, A. Santos, J. Ros, J. Organomet. Chem. 309 (1986) 169.
[24] Y. Fan, I.P.-C. Liu, P.E. Fanwick, T. Ren, Organometallics 28 (2009) 3959.
[25] F. Paul, C. Lapinte, Coord. Chem. Rev. 178–180 (1998) 431.
[26] J.-L. Fillaut, N.N. Dua, F. Geneste, L. Toupet, S. Sinbandhit, J. Organomet. Chem. 691 (2006) 5610.
[27] N. Ahmad, J.J. Levison, S.D. Robinson, M.F. Uttley, E.R. Wonchoba, G.W. Parshall, Inorg. Synth. 15 (1974) 45.
[28] H.L. Bruce, L.A. Craig, J. Am. Chem. Soc. 119 (1997) 4555.
[29] G.G.A. Balavonine, G. Doisneau, T. Fillebeen-khan, J. Organomet. Chem. 412 (1991) 381.
[30] J.A. Mata, S. Uriel, R. Llusar, E. Peris, Organometallics 19 (2000) 3797.
[31] G.M. Sheldrick, SHELXS-97, Program for X-Ray Crystal Structure Solution, University of Göttingen, Göttingen, Germany, 1997.
[32] G.M. Sheldrick, SHELXL-97, A Program for Crystal Structure Refinement, University of Göttingen, Göttingen, Germany, 1997.